Applied Physics Express

Thermal defect healing of single-walled carbon nanotubes assisted by supplying carbon-containing reactants

To cite this article before publication: Mengyue Wang *et al* 2022 *Appl. Phys. Express* in press https://doi.org/10.35848/1882-0786/acaaec

Thermal defect healing of single-walled carbon nanotubes assisted by supplying carbon-containing reactants

Mengyue Wang, [*a] *Manaka Maekawa,* [a] *Man Shen,* [a] *Yuanjia Liu,* [a] *Michiharu Arifuku,* [b] *Noriko Kiyoyanagi,* [b] *Taiki Inoue,* [a] *Yoshihiro Kobayashi*[*a]

[a] Department of Applied Physics, Osaka University, Suita, Osaka 565-0871, Japan

[b] Nippon Kayaku Co., Ltd., 31-12, Shimo 3-chome, Kita-ku, Tokyo 115-8588, Japan

*Email: wang.my@ap.eng.osaka-u.ac.jp, kobayashi@ap.eng.osaka-u.ac.jp

Abstract:

We experimentally investigated the effect of carbon-containing reactants (C_2H_2) on healing the defects in single-walled carbon nanotubes (SWCNTs) by thermal processes at high temperatures (~1100°C). Introducing C_2H_2 notably improved the crystallinity of healed SWCNTs compared with the thermal process in Ar ambient without C_2H_2. The defect healing rate increased with increasing C_2H_2 partial pressure and the healing effect of C_2H_2 was more remarkable for relatively thinner SWCNTs (<1.1 nm). Combined with the relevant theoretical works reported previously, we propose the healing model, in which C_2H_2 helps to heal the vacancy defects and increases the healing rate at high temperatures.

Keywords: single-walled carbon nanotubes, defect healing, crystallinity, post treatment, C_2H_2

Carbon nanotubes (CNTs),[1] have been wildly studied because of their supposed outstanding electronic,[2] optical,[3] and mechanical[4] properties. Compared to multiwalled CNTs (MWCNTs), single-walled CNTs (SWCNTs) becomes one of the potential materials for application in electronics,[5] sensors,[6] and so on. However, the defects formed in SWCNTs dramatically degrade the electrical[7] and thermal transport[8] and mechanical strength[9] of SWCNTs. Such defects, including adatom,[10] vacancy,[11] pentagon-heptagon pair (5|7) defects,[12] can be created in the SWCNT growth process [13-15] and chemical post-treatment step.[16]

High-temperature treatment has been suggested to heal the defects.[17] During the SWCNT growth process, the highly crystalline SWCNTs tends to form in high temperature synthesis procedure.[18] Theoretical and experimental studies explained this phenomenon by the temperature-activated catalytic defect healing,[19] which mentioned that simple defects with lower healing activation energy would be more readily cured, such as the 5|7 defects.[12] Besides, the high temperature was also applied to the post-treatment process to heal the low-temperature synthesized or chemically treated CNTs. For example, treating MWCNTs at 1200–2000 ^{o}C in a high vacuum or at 2000–2800 ^{o}C in an argon (Ar) atmosphere improved crystallinity.[20-22] Similarly, in SWCNT healing, high-temperature treatment (1000–2400 ^{o}C) has also been reported to increase the overall crystallinity.[23, 24] Nevertheless, there appears to be a limitation in healing vacancy defects at high temperature. Based on the simulation studies, once the vacancy defects formed and diffused into nanotubes, even if the vacancy defects could proceed with a self-healing via ring isomerization, it is hard to heal entirely unless foreign carbon atoms are added.[25] In previous studies, ethanol has been used as the defect healer in the restoration of graphene oxide.[26, 27] Recently, simulation studies proved that the carbon-containing reactants (CO, C_2H_2 and C_2H_4) are good candidates to heal vacancy defects during high-temperature CNT synthesis.[25, 28-30] Unfortunately, there is still no experimental report on the healing effect of such carbon-containing reactants.

In this research, we experimentally present the healing effect of carbon-containing reactants on the defective SWCNTs. As one of the carbon-containing reactants, C_2H_2 is selected because it does not contain oxygen atoms, which lead to spontaneous formation of oxidants during pyrolysis process and disturb the healing result. To decrease

the metal impurities and avoid the formation of additional defects during post-treatment, we selected the solid carbon nanoparticles as the growth seed.[31, 32] Through structure characterization, we explored the influence of C_2H_2 partial pressure on annealing process. Besides, SWCNTs diameter dependent healing efficiency is discussed. Noticeably, the injection of C_2H_2 increased the healing efficiency, and it showed a significant increase in the thin SWCNTs.

Relatively defective SWCNTs were prepared by lowering growth temperature from the optimized condition in our previous study.[33] As the starting material of growth seeds, ~10 nm diameter purified ND particles were dropped on the ozone-cleaned Si substrates with a 300-nm-thick thermal oxide layer. The ND pretreatment and the SWCNT growth were performed in a quartz tube chamber which is held in a tubular CVD furnace (GE-1000, GII Techno).[33] Before the growth of SWCNTs, the ND was pretreated with the surface-cleaning process and the annealing procedure.[33] After the annealing process, SWCNTs were synthesized for 10 min with a mixture of 10-sccm C_2H_2 (2%)/Ar and 10-sccm H_2 (3%)/Ar. The total pressure was kept at 500 Pa, corresponding to a C_2H_2 partial pressure of 5 Pa. The temperature of the three-zone furnace was set with a gradient, 850-785-750 °C, which corresponds to the temperature of gas mixture preheating, SWCNT growth (substrate temperature), and post heating, respectively.

Then, the heat treatment for the defect healing was proceeded. The annealing temperature was set at 1000 or 1100 °C to ensure the healing of defects in Ar ambient and the pyrolysis of C_2H_2.[20-22, 34] The healing time was varied from 0 min to 90 min, where the 0 min represents the healing process stopped once the substrate temperature arrived at healing temperature. During the temperature rising process, 250-sccm Ar was injected. When the temperature arrived at the annealing temperature, the gas flow was switched to a 250-sccm mixture of Ar (235–250 sccm) and C_2H_2 (2%)/Ar (0–15 sccm). The total pressure was 220 Pa, corresponding to a C_2H_2 partial pressure of 0-0.264 Pa, which limits the deposition of amorphous carbon (a-C) and is lower than the value needed for the nucleation of CNTs (0.5 Pa).[33] To confirm the deposition of a-C, we used the same cleaned Si substrates without any growth seeds and SWCNTs as a reference (hereafter called blank samples).

The structure of the SWCNTs before and after the healing process was analyzed by Raman spectroscopy. A Raman spectrometer (LabRAM HR800, HORIBA Jovin Yvon) was used with an excitation wavelength λ_{ex} of 633 nm. Raman spectra of 30 randomly selected spots were collected from each sample, and the averaged spectra were used for the analysis. The quality of formed SWCNTs was evaluated using the intensity ratio of the G-band (~1590 cm^{-1}) to the D-band (1330–1360 cm^{-1}), which was represented as I_G/I_D. The SWCNT quantity was evaluated by comparing the intensity ratio of the G-band with the peak from Si substrates (~520 cm^{-1}), which was represented as I_G/I_{Si}. Scanning electron microscopy (SEM) (S-4800, Hitachi) was used for morphology observations of SWCNTs with an acceleration voltage of 5 kV.

To investigate the healing role of C_2H_2, we analyzed the SWCNT samples annealed at 1100 °C with 0, 0.035, 0.088, 0.176, and 0.264 Pa of C_2H_2 injection. The healing time was varied from 0 to 90 min. As shown in Figure S1, a control experiment was conducted to exclude the possibility of new nucleation of CNTs. Thus, the increase in the Raman spectra intensity of the annealed SWCNT samples results from the healing effect.

The radial breathing modes (RBMs) of Raman spectra changed with healing time and the partial pressure of C_2H_2 are exhibited in Figure 1 (a). As a representative, G-band and D-band of the SWCNT samples annealed with 0.088 Pa-C_2H_2 is shown in Figure 1(b). Compared with the pristine SWCNTs, the RBM, G-band, and D-band intensity first decreased during the temperature rising process (at 0 min) presumably because SWCNTs were damaged by the interaction between the substrate and SWCNTs [35]. Similar decrease also appeared in the 1000 °C healing experiments and was explained in the Supporting information (Figure S2). By prolonging the healing time to 60 min, the intensity of RBM spectra and G-band in Figure 1 gradually increased both with and without the use of C_2H_2. Additional Raman spectra of SWCNTs healed with 0.035 and 0.088 Pa-C_2H_2 are shown in Figure S3. Without the use of carbon-containing reactant, such increase of G-band and RBM intensity at high temperature was explained by the healing of defects.[23, 24, 36, 37] Here, the use of C_2H_2 caused a more rapid intensity increase of the RBM peaks at around 210 and 280 cm^{-1}.

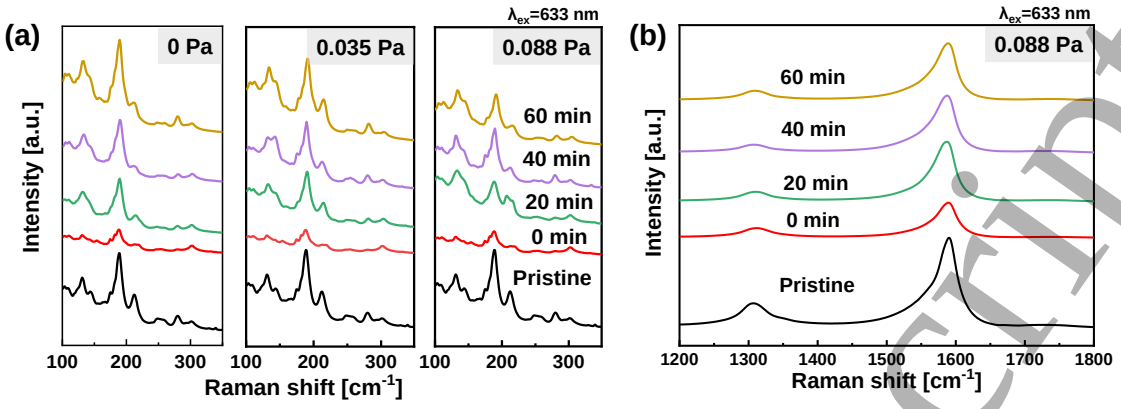

Figure 1: (a) RBM spectra of the pristine SWCNTs and the healed SWCNTs treated with 0, 0.035, and 0.088 Pa C_2H_2 at 1100 °C for different time. (b) G-band and D band of the pristine SWCNTs and the SWCNTs annealed with 0.088 Pa C_2H_2 at 1100 °C.

The Raman spectra and the SEM images of the healed SWCNTs with further changing the C_2H_2 partial pressure is exhibited in Figure S4 and S5. As a representative, the SEM images of the pristine SWCNTs and SWCNTs healed with 0.035 Pa-C_2H_2 are shown in Figure 2. As shown in the Raman spectra, injecting C_2H_2 with a low partial pressure (0.035 Pa) helped to increase I_G/I_D ratio. When increasing the C_2H_2 partial pressure, deposition of a-C was observed by SEM.

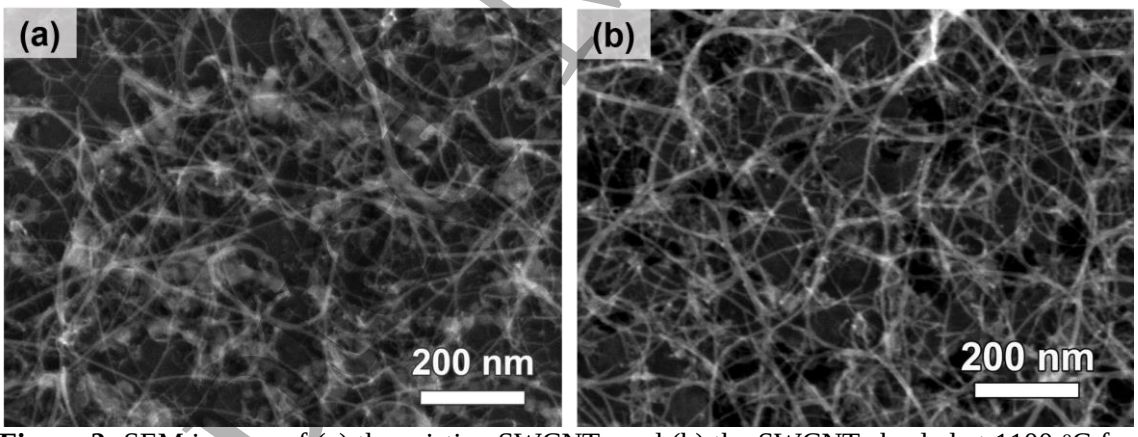

Figure 2: SEM images of (a) the pristine SWCNTs and (b) the SWCNTs healed at 1100 °C for 60 min with 0.035 Pa C_2H_2.

To further analyze the change in defect density during the healing process, we calculate the I_G/I_D ratio of the SWCNTs healed with different healing time (Figure 3). As the time went by, the SWCNTs healed with C_2H_2 gradually expressed higher I_G/I_D ratio than the SWCNTs healed without C_2H_2, which reflects the higher crystallinity of

SWCNTs. Moreover, different defect healing rates appeared with changing C_2H_2 partial pressure. In 0 and 0.035 Pa-C_2H_2 injected process, the defect healing rate was similar in first 20 min. After 20 min, compared with the 0 Pa-C_2H_2 case, a higher overall healing rate from 20 min to 60 min was found in the 0.035 Pa case, and the I_G/I_D ratio finally increased to ~8. By further raising the partial pressure of C_2H_2 to 0.088 Pa, a more noticeable increase in healing rate appeared in the first 20 min, and the I_G/I_D ratio reached ~8.9 at 40 min. When prolonging the healing time to 60 min, however, we noticed that the I_G/I_D ratio decreased. According to Figure S6, the I_G/I_{Si} ratio kept stable for 20 min and the I_D/I_{Si} ratio of the blank samples gradually increased, which represents the deposition of a-C. Thus, the decrease of I_G/I_D ratio for long healing time in the 0.035 and 0.088 Pa cases can be attributed to a-C deposition.

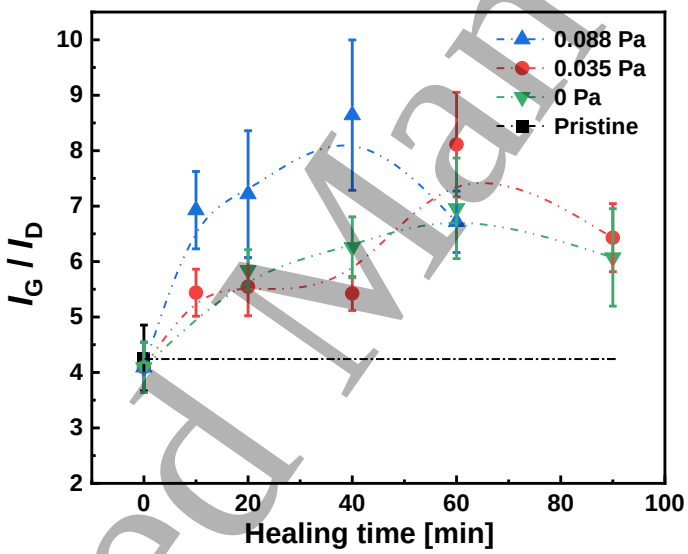

Figure 3: Change in the I_G/I_D ratio of the SWCNTs along the healing time with different C_2H_2 partial pressure at 1100 °C.

Then, we further discuss the influence of C_2H_2 injection to the healing rate of SWCNTs with different diameters. The SWCNT diameter (d_t) is related to the RBM wavenumber (ω_{RBM}) according to the equation:[38)]

$$\omega_{RBM}\ (cm^{-1}) = 223.5\ /d_t\ (nm) + 12.5$$

Thus, the high wavenumber (200-300 cm^{-1}) of RBM corresponds to the thin SWCNTs (<1.1 nm), and the low wavenumber (100–200 cm-1) represents the thick SWCNTs (>1.1

nm). Among the RBM spectra shown in Figure 1 (a), significant intensity change appears on the four peaks at around 133, 188, 210, and 280 cm^{-1}, which corresponds to the diameter of 1.8, 1.3, 1.1 and 0.8 nm, respectively. Taking the above four peaks as the representative, the healing rates are determined as shown in Figure 4. The related details of calculation and normalized RBM intensity varied with the healing time are exhibited in Figure S7. As reported by previous works,[12, 39, 40] the low formation energy eases the formation of vacancy defects in thin SWCNTs. Healing such defects in thin SWCNTs would take longer time compared with thick SWCNTs. Thus, without C_2H_2, slow healing rate is found in the thin SWCNTs. When C_2H_2 was added, the healing rate increased more drastically for the thin SWCNTs. This phenomenon confirms that the injection of C_2H_2 enhanced the defect healing especially for the thin SWCNTs.

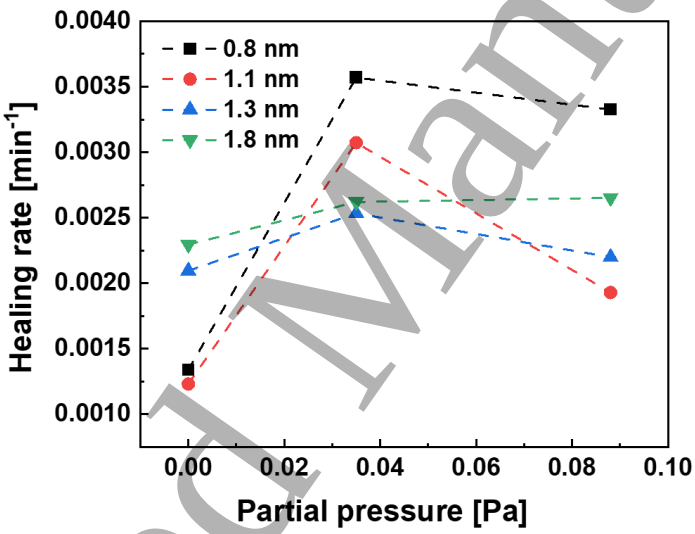

Figure 4: Change in the healing rate with the partial pressure of C_2H_2 for the SWCNTs with different diameter at 1100 °C.

Based on the results of C_2H_2-injected defect healing, we derived the healing behavior of C_2H_2 and schematically depicted it in Figure 5. During the high temperature healing process with the presence of trace amount of oxidative gas impurities (O_2, H_2O, or CO_2), the adatom defects could be partly healed through etching reaction.[41] Theoretical studies suggested that carbon-containing reactant is effective to heal vacancy defects because such reactant can adsorbed on the defect sites and incorporated into a lattice of SWCNTs.[25, 28-30] Thus, in Figure 5, adatom and vacancy defects are the representative defects in the healing process.

Because of the low formation energy, adatom defect is easy to construct and appears with higher density compared with vacancy defects.[39] Besides, related to a diameter of SWCNTs, the formation energy of defects is low in thin SWCNTs,[12, 40] which eases vacancy defect formation in thin SWCNTs. Therefore, as shown in Figure 5, higher-density vacancy defects appear in the pristine thin SWCNTs. High defect density takes longer time to be healed, which brings about low healing rates for thin SWCNTs.

When only heated in Ar gas, adatom defects were partly healed while vacancy defects were kept. When C_2H_2 was added, the vacancy defects could be better healed, causing an increase in healing rate. Especially for thin SWCNTs, the healing rate was drastically increased. Moreover, the pyrolysis of C_2H_2 produced H_2, and it helped to remove adatom defects.[41]

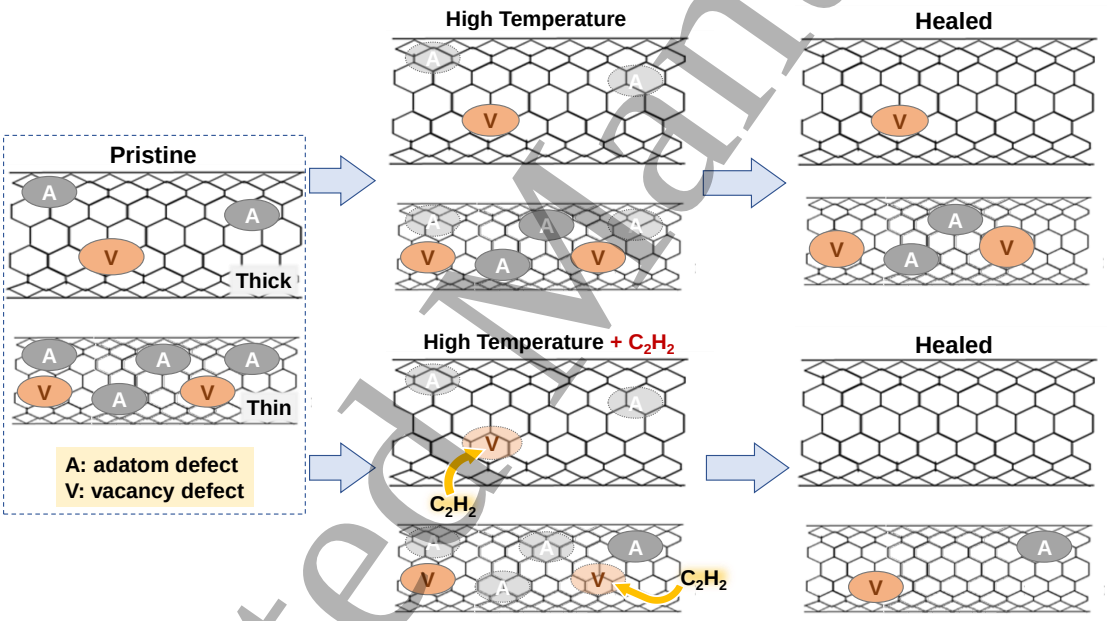

Figure 5: Schematic defect healing diagram of the pristine SWCNTs annealed with or without the injection of C_2H_2. The pristine SWCNTs are divided into thick (>1.1 nm) and thin (<1.1nm) SWCNTs according to their diameter.

Besides, we also investigated the healing effect of ethylene (C_2H_4). As shown in Figure S8, the injection of C_2H_4 resulted in the efficient healing of SWCNTs similarly to the case of C_2H_2, indicating the general effectiveness of carbon-containing reactants in thermal defect healing.

In conclusion, we experimentally confirmed the healing behavior of C_2H_2 in the high temperature annealing process, which had been only analyzed through theoretical methods. Compared with the SWCNTs healed in Ar gas, the SWCNTs healed with C_2H_2 presented higher crystallinity. The defect healing rate was increased with rising the partial pressure of C_2H_2 from 0 to 0.088 Pa. Further, we found that the healing effect of C_2H_2 was more evident in the thin SWCNTs (<1.1 nm). Combining with the previous simulation research, we consider that C_2H_2 helps to heal the vacancy defects and increases the high temperature healing rate. Moreover, we also found that C_2H_4 exhibited a healing ability which is similar to C_2H_2. These results prove that injecting carbon-containing reactants, would be an additional important factor for healing SWCNT defects with high efficiency. With the assistance of such reactants, SWCNTs with higher crystallinity can be achieved by the post treatment process, which would further realize the improvement of SWCNT properties required for electronic, thermal, and mechanical applications.

Acknowledgement

We thank Dr. T. Sakata of Research Center for Ultra-High Voltage Electron Microscopy, Osaka University, for assistance in the SEM observation. The part of this work was financially supported by JSPS KAKENHI (Grant Numbers JP15H05867 and JP17H02745).

References

1) S. Iijima, *Nature* **354**, 56 (1991).
2) G. D. Nessim, *Nanoscale* **2**, 1306 (2010).
3) M. J. O'Connell, S. M. Bachilo, C. B. Huffman, V. C. Moore, M. S. Strano, E. H. Haroz, K. L. Rialon, P. J. Boul, W. H. Noon, C. Kittrell, J. Ma, R. H. Hauge, R. B. Weisman, R. E. Smalley, *Science* **297**, 593 (2002).
4) Y. Bai, H. Yue, R. Zhang, W. Qian, Z. Zhang, F. Wei, *Acc. Mater. Res.* **2**, 998 (2021).

5) A. D. Franklin, M. Luisier, S.-J. Han, G. Tulevski, C. M. Breslin, L. Gignac, M. S. Lundstrom, W. Haensch, *Nano Lett.* **12**, 758 (2012).
6) T. Yamada, Y. Hayamizu, Y. Yamamoto, Y. Yomogida, A. Izadi-Najafabadi, D. N. Futaba, K. Hata, *Nat. Nanotechnol.* **6**, 296 (2011).
7) S. Suzuki, Y. Kobayashi, *Jpn. J. Appl. Phys.* **44**, L1498 (2005).
8) T. Yamamoto, K. Watanabe, *Phys. Rev. Lett.* **96**, 255503 (2006).
9) M. Sammalkorpi, A. Krasheninnikov, A. Kuronen, K. Nordlund, K. Kaski, *Phys. Rev. B* **70**, 245416 (2004).
10) L. Tsetseris, S. T. Pantelides, *Carbon* **47**, 901 (2009).
11) J. Y. Huang, F. Ding, B. I. Yakobson, *Phys. Rev. B* **78**, 155436 (2008).
12) Q. Yuan, Z. Xu, B. I. Yakobson, F. Ding, *Phys. Rev. Lett.* **108**, 245505 (2012).
13) Y. Xia, Y. Ma, Y. Xing, Y. Mu, C. Tan, L. Mei, *Phys. Rev. B* **61**, 11088 (2000).
14) J. C. Burgos, E. Jones, P. B. Balbuena, *J. Phys. Chem. C* **118**, 4808 (2014).
15) W. Qian, T. Liu, F. Wei, Z. Wang, G. Luo, H. Yu, Z. Li, *Carbon* **41**, 2613 (2003).
16) M. C. Hersam, *Nat. Nanotechnol.* **3**, 387 (2008).
17) P. Vinten, P. Marshall, J. Lefebvre, P. Finnie, *J. Phys. Chem. C* **117**, 3527 (2013).
18) C. J. Lee, J. Park, Y. Huh, J. Yong Lee, *Chem. Phys. Lett.* **343**, 33 (2001).
19) R. Zhang, Y. Zhang, F. Wei, *Acc. Chem. Res.* **50**, 179 (2017).
20) D. Mattia, M. P. Rossi, B. M. Kim, G. Korneva, H. H. Bau, Y. Gogotsi, *J. Phys. Chem. B* **110**, 9850 (2006).
21) R. Jin, Z. X. Zhou, D. Mandrus, I. N. Ivanov, G. Eres, J. Y. Howe, A. A. Puretzky, D. B. Geohegan, *Phys. B* **388**, 326 (2007).
22) J. Zhao, Y. Zhang, Y. Su, X. Huang, L. Wei, E. S.-W. Kong, Y. Zhang, *Diamond Relat. Mater.* **25**, 24 (2012).
23) M. Yudasaka, H. Kataura, T. Ichihashi, L. C. Qin, S. Kar, S. Iijima, *Nano Lett.* **1**, 487 (2001).
24) M. Yudasaka, T. Ichihashi, D. Kasuya, H. Kataura, S. Iijima, *Carbon* **41**, 1273 (2003).
25) T. Nongnual, J. Limtrakul, *J. Phys. Chem. C* **115**, 4649 (2011).

26) K. K. H. De Silva, H.-H. Huang, S. Suzuki, R. Badam, M. Yoshimura, *Jpn. J. Appl. Phys.* **57**, 08NB03 (2018).
27) C.-Y. Su, Y. Xu, W. Zhang, J. Zhao, A. Liu, X. Tang, C.-H. Tsai, Y. Huang, L.-J. Li, *ACS Nano* **4**, 5285 (2010).
28) B. Xiao, J.-x. Zhao, Y.-h. Ding, C.-c. Sun, *ChemPhysChem* **11**, 3505 (2010).
29) B. Xiao, X.-f. Yu, Y.-h. Ding, *J. Mol. Model.* **20**, 2125 (2014).
30) R. L. Zhou, H. Y. He, B. C. Pan, *Phys. Rev. B* **75**, 113401 (2007).
31) D. Takagi, Y. Kobayashi, Y. Homma, *J. Am. Chem. Soc.* **131**, 6922 (2009).
32) Y. Homma, H. Liu, D. Takagi, Y. Kobayashi, *Nano Res.* **2**, 793 (2009).
33) M. Wang, K. Nakamura, M. Arifuku, N. Kiyoyanagi, T. Inoue, Y. Kobayashi, *ACS Omega* **7**, 3639 (2022).
34) N. Matsumoto, A. Oshima, G. Chen, M. Yudasaka, M. Yumura, K. Hata, D. N. Futaba, *Carbon* **87**, 239 (2015).
35) P. Nemes-Incze, G. Magda, K. Kamarás, L. P. Biró, *Nano Res.* **3**, 110 (2010).
36) L. G. Cançado, A. Jorio, E. H. M. Ferreira, F. Stavale, C. A. Achete, R. B. Capaz, M. V. O. Moutinho, A. Lombardo, T. S. Kulmala, A. C. Ferrari, *Nano Lett.* **11**, 3190 (2011).
37) Y. Yang, C. Ramirez, X. Wang, Z. Guo, A. Tokranov, R. Zhao, I. Szlufarska, J. Lou, B. W. Sheldon, *Carbon* **115**, 402 (2017).
38) S. M. Bachilo, M. S. Strano, C. Kittrell, R. H. Hauge, R. E. Smalley, R. B. Weisman, *Science* **298**, 2361 (2002).
39) F. Ding, *Phys. Rev. B* **72**, 245409 (2005).
40) A. J. Lu, B. C. Pan, *Phys. Rev. Lett.* **92**, 105504 (2004).
41) L. Tsetseris, S. T. Pantelides, *J. Phys. Chem. B* **113**, 941 (2009).

Supporting information

Thermal defect healing of single-walled carbon nanotubes assisted by supplying carbon-containing reactants

Mengyue Wang, [*a] *Manaka Maekawa,* [a] *Man Shen,* [a] *Yuanjia Liu,* [a] *Michiharu Arifuku,* [b]

Noriko Kiyoyanagi, [b] *Taiki Inoue,* [a] *Yoshihiro Kobayashi*[*a]

[a] Graduate school of engineering, Osaka University, Suita, Osaka 565-0871, Japan

[b] Nippon Kayaku Co., Ltd., 31-12, Shimo 3-chome, Kita-ku, Tokyo 115-8588, Japan

*Email: kobayashi@ap.eng.osaka-u.ac.jp

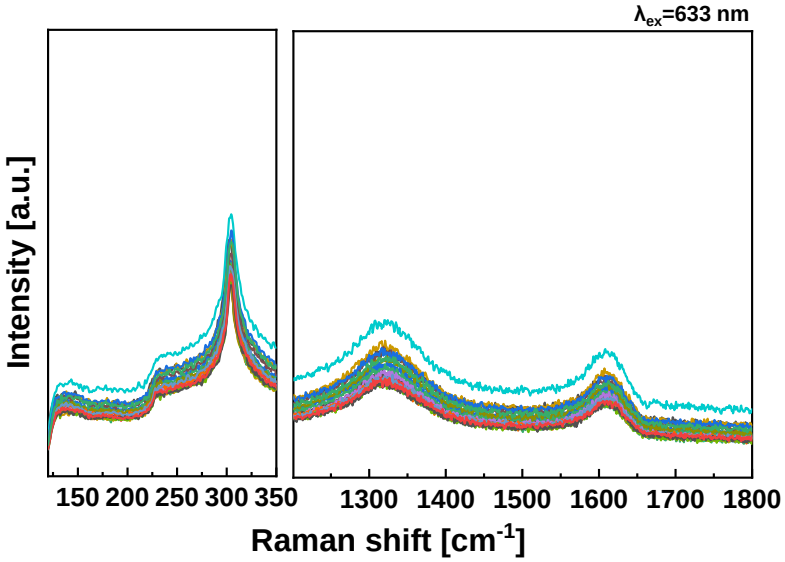

Figure S1: Raman spectra of the nanodiamond (ND) sample treated with the same thermal process as SWCNT growth but without the injection of carbon source and then the healing process (heated at 1100 °C for 60 min with 0.088 Pa C_2H_2 injection).

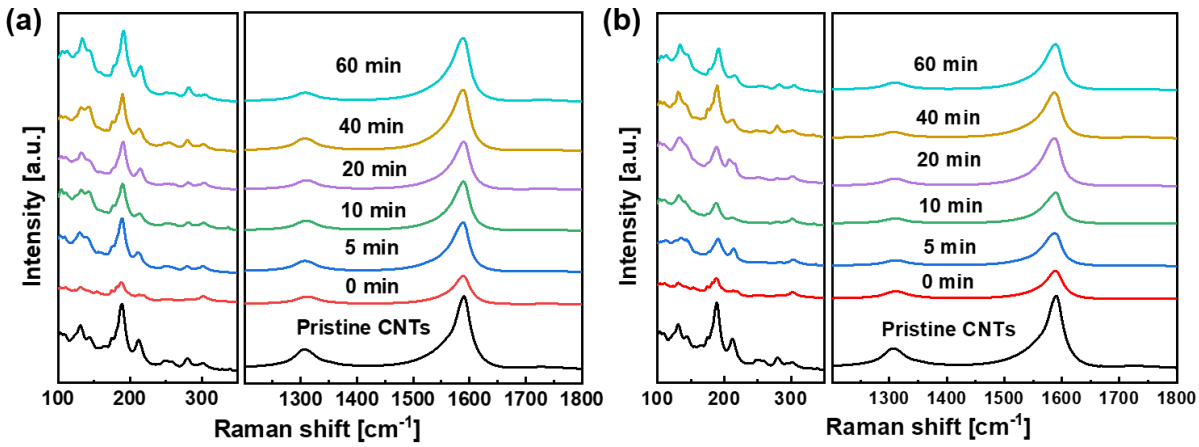

Figure S2: Raman spectra of the pristine SWCNTs and the healed SWCNTs treated with (a) 0.035, and (b) 0.088 Pa C_2H_2 for 0, 5, 10, 20, 40, and 60 min at 1100 °C.

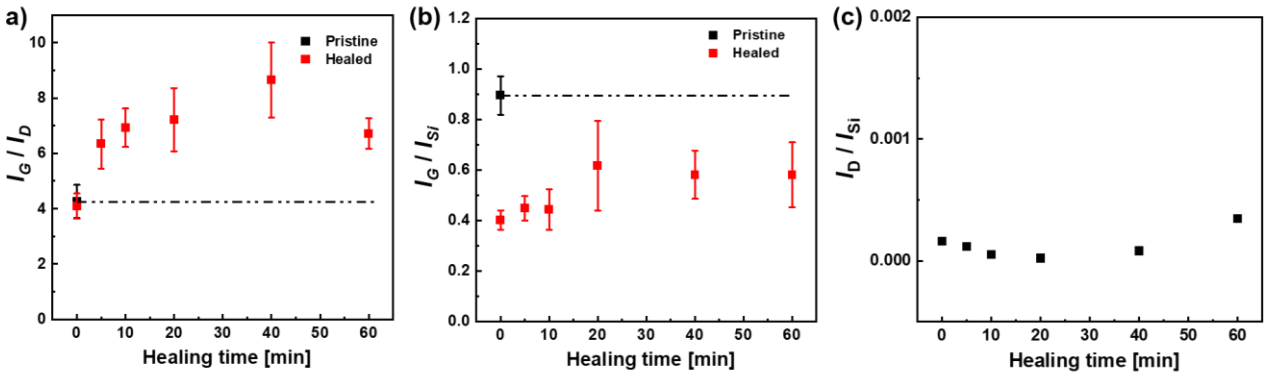

Figure S3: Process time dependence of the (a) I_G/I_D ratio and (b) I_G/I_{Si} ratio of the SWCNTs, and (c) the I_D/I_{Si} ratio of the relevant blank sample treated with the C_2H_2-injected healing process (0.088 Pa). The I_G/I_D and I_G/I_{Si} ratios of the pristine SWCNTs were plotted as a reference.

.

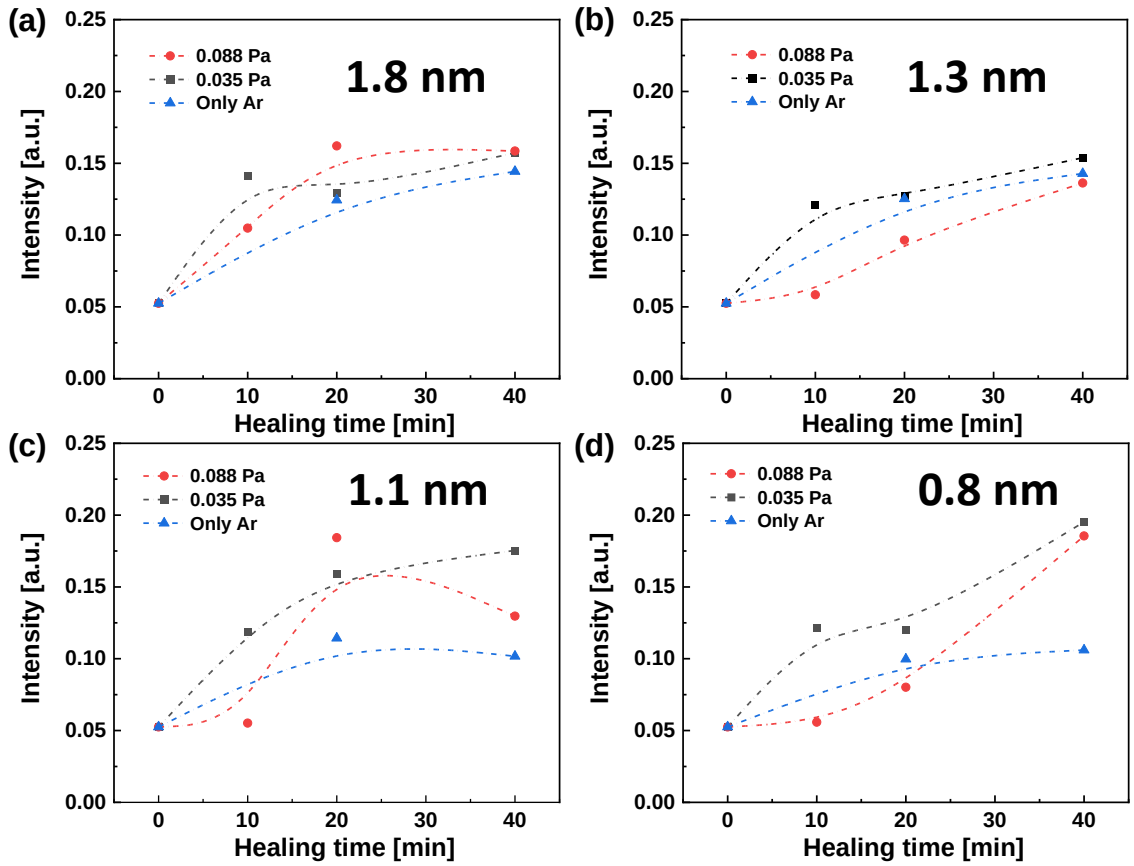

Figure S4: The changes in the RBM peak intensity along the healing time (0, 10, 20, and 40 min). The four representative RBM peaks correspond to the SWCNTs with different diameter: (a) 1.8, (b) 1.3, (c) 1.1, and (d) 0.8 nm.

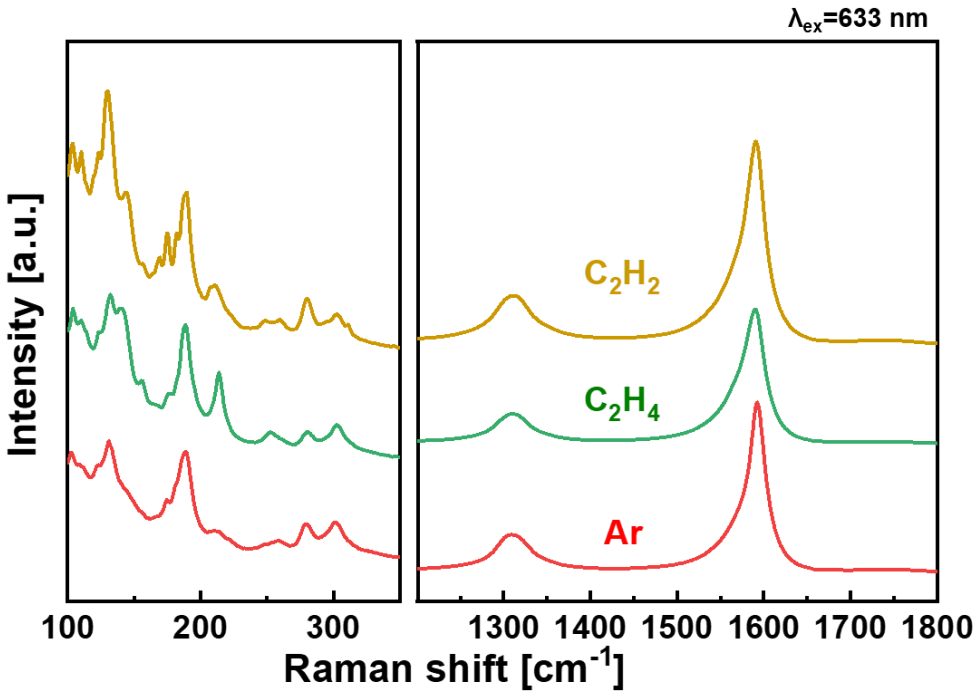

Figure S5: Raman spectra of the healed SWCNTs treated with only Ar, 0.352 Pa C_2H_2 and 0.352 Pa C_2H_4 for 60 min at 1100 ºC.